SYNTHESIS AND CHARACTERIZATION OF γ-MnO_2 FROM $LiMn_2O_4$

M. M. THACKERAY*, A. DE KOCK and L. A. DE PICCIOTTO

Division of Materials Science and Technology, CSIR, P.O. Box 395, Pretoria 0001 (South Africa)

G. PISTOIA

Centro di Studio per la Elettrochimica e la Chimica Fisica delle Interfasi, CNR, Rome (Italy)

Summary

γ-MnO_2 can be synthesized by acid treatment of the spinel $LiMn_2O_4$; it is formed via an intermediate λ-MnO_2 phase. The γ-MnO_2 phase is significantly more crystalline and contains less occluded water than electrolytically prepared MnO_2 (EMD). Unlike EMD, the occluded water can be removed almost entirely by heating the γ-MnO_2 phase to 300 °C. Heating to 300 °C causes a transformation of the γ-MnO_2 structure to a predominantly β-MnO_2 phase. The discharge capacity of the β-phase in room-temperature lithium cells is comparable with the capacity of the γ/β-MnO_2 phase which is formed by heating EMD to 350 - 420 °C. Lithium-ion diffusion rates in the γ-MnO_2 and β-MnO_2 phases derived from the spinel precursor were determined to be 1×10^{-9} cm^2 s^{-1} and 2×10^{-10} cm^2 s^{-1}, respectively.

Introduction

Li/MnO_2 batteries play a small, but significant, role in the world's battery industry. The manganese dioxide that is used predominantly in these batteries is prepared electrolytically (EMD). EMD has a γ-type structure which is generally regarded to be an intergrowth of a rutile- and a ramsdellite-type structure. EMD contains, typically, 5 wt.% H_2O which must be removed from the structure to ensure effective operation and long life of the battery. Heat-treatment of EMD to 350 - 420 °C removes about 80% of the water and causes a transformation of the γ-MnO_2 structure to a γ/β-MnO_2 phase [1]. During discharge of the battery, Li^+ ions are inserted into, and reduce, the γ/β-MnO_2 phase to yield the product Li_xMnO_2 ($0 < x < 1$) [2]. This type of battery cannot be recharged or cycled to any useful extent.

Considerable attention has been given recently to the application of the spinel-related manganese dioxide phase, λ-MnO_2, in lithium batteries.

*Author to whom correspondence should be addressed.

0378-7753/89/$3.50

λ-MnO_2 is an anhydrous product which can be prepared at room temperature by lithium extraction from the spinel $Li[Mn_2]O_4$ [3]; it has the $[Mn_2]O_4$ spinel-framework structure. Lithium can also be inserted into $Li[Mn_2]O_4$. Powder X-ray and neutron diffraction data have shown that the $[Mn_2]O_4$ spinel framework remains intact over a wide compositional range, $Li_x[Mn_2]O_4$ ($0 < x < 2$) [3 - 6]. Cyclic voltammetry studies have shown that lithium may be cycled in, and out of, λ-MnO_2, thereby rendering this material an attractive electrode for a secondary lithium battery [7]. Although lithium extraction from $Li[Mn_2]O_4$ occurs readily in acid at 25 °C [3], electrochemical extraction beyond $Li_{0.5}[Mn_2]O_4$ appears to be difficult [8].

It has been reported recently that acid digestion of λ-MnO_2 transforms the $[Mn_2]O_4$ spinel framework into a γ-MnO_2 product with an anomalously low water content [9]. The water can be almost entirely removed by heat treatment to 300 °C. However, this heat treatment causes a transformation of the γ-phase to a structure with predominant β-MnO_2 characteristics.

It has been established that β-MnO_2 with a well-developed rutile structure does not exhibit good electrochemical activity in lithium cells [10]; a maximum uptake of 0.2 Li^+ ions per β-MnO_2 unit has been reported [11]. By contrast, it has been found that the β-MnO_2 phase derived from a λ-MnO_2 precursor shows surprisingly good electrochemical activity in lithium cells. The electrochemical properties of this β-phase are reported in this paper and compared with the performance of standard heat treated EMD samples.

Experimental

The preparation of λ-MnO_2 and γ-MnO_2 by reacting $LiMn_2O_4$ with 0.5 M H_2SO_4 has been reported in detail elsewhere [9].

The water content of MnO_2 samples was calculated from their $[H^+]$ concentration, which was determined by gravimetric methods (0.1 wt.% $[H^+]$ corresponds to approximately 1.0 wt.% H_2O). A Malvern Instruments Master Particle Sizer M3.0 was used to obtain particle-size distributions in the MnO_2 samples. Powder X-ray diffraction patterns were recorded on an automated Rigaku diffractometer with Cu Kα radiation, monochromated by a curved graphite crystal. Lithium-ion diffusion rates ($\tilde{D}$) in MnO_2 samples were determined by a method described by Basu and Worrell [12], with a Princeton Applied Research (PAR) Model 173 potentiostat/galvanostat coupled to a Model 175 programmer. The slopes of the open-circuit voltage curves required for the diffusion measurements were obtained from Li/MnO_2 cells between the compositional limits $x = 0.02$ and $x = 0.08$ in Li_xMnO_2. Lithiated MnO_2 cathodes were considered to have equilibrated when the cell voltage varied by less than 1 mV in 24 h. Electrochemical tests were carried out in two separate laboratories in cells of the type:

Li/1 M $LiClO_4$ in PC, DME*/MnO_2

*PC = propylene carbonate; DME = dimethoxyethane.

Details of cell construction are given elsewhere [13, 14]. At the CSIR (South Africa) cells were discharged at constant current at low rates, typically at 30 μA cm^{-2}. At the CNR (Italy), the discharge capacity and cycling behaviour of cells containing spinel-derived β-MnO_2 and standard EMD cathodes were compared at a higher current density (1 mA cm^{-2}); in these cells 20 wt.% Teflon acetylene black (TAB) was added to the cathode to improve the electronic conductivity and strength of the compacted MnO_2 electrode.

Results and discussion

The reaction conditions used for the preparation of some selected MnO_2 samples from $LiMn_2O_4$, heat treatment temperatures and $[H^+]$ values, as reported in ref. 9, are given in Table 1. The $[H^+]$ concentrations in EMD samples and heated products are also tabulated for comparison. Powder X-ray diffraction patterns of $LiMn_2O_4$, λ-MnO_2 and a standard, anhydrous β-MnO_2 sample, prepared by decomposing $Mn(NO_3)_2$ in air at 400 °C [15], are shown in Fig. 1(a) - (c). X-ray patterns of a γ-MnO_2 sample derived from $LiMn_2O_4$, EMD, and their heat treated products are given in Fig. 2(a) - (c) and Fig. 3(a) - (c).

Lithium extraction from $LiMn_2O_4$ at 25 °C yields the anhydrous, highly crystalline λ-MnO_2 phase [3]. The structure of λ-MnO_2 has been well characterized [5, 6]; it has the $[Mn_2]O_4$ spinel framework, as evident from the strong similarity in the powder X-ray diffraction patterns of λ-MnO_2 and $LiMn_2O_4$ (Fig. 1(a) and (b)). If the reaction temperature is raised to 40 °C and the reaction time with acid is extended (Table 1), a γ-MnO_2 product is

TABLE 1

Reaction conditions used for the preparation of various MnO_2 samples from $LiMn_2O_4$ in 0.5 M H_2SO_4 [9]

Starting material	Reaction temp. (°C)	Reaction time (days)	Heat treatment (°C)	End-product	$[H^+]$ (wt.%)
$LiMn_2O_4$	25	4	75	λ-MnO_2	0.03
$LiMn_2O_4$	40	13	75	γ-MnO_2	0.13
$LiMn_2O_4$	40	13	200	γ-MnO_2	0.09
$LiMn_2O_4$	40	13	300	β-MnO_2	0.02
$LiMn_2O_4$	40	13	350	β-MnO_2	0.01
EMD (IC 1)	—	—	75	γ-MnO_2	0.50
EMD (IC 1)	—	—	350	γ/β-MnO_2	0.07
EMD (Delta)*	—	—	75	γ-MnO_2	0.50
EMD (Delta)	—	—	350	γ/β-MnO_2	0.10
EMD (Delta)	—	—	420	γ/β-MnO_2	0.09

*Obtained from Delta (EMD) (Pty) Ltd, Nelspruit, South Africa.

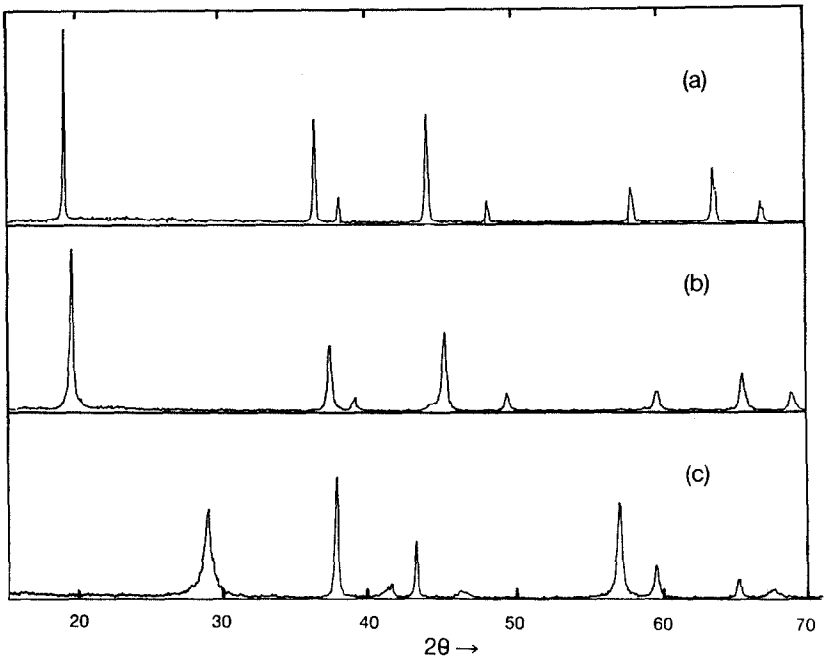

Fig. 1. Powder X-ray diffraction patterns of (a) $LiMn_2O_4$; (b) λ-MnO_2; (c) a standard, anhydrous β-MnO_2 sample prepared from $Mn(NO_3)_2$.

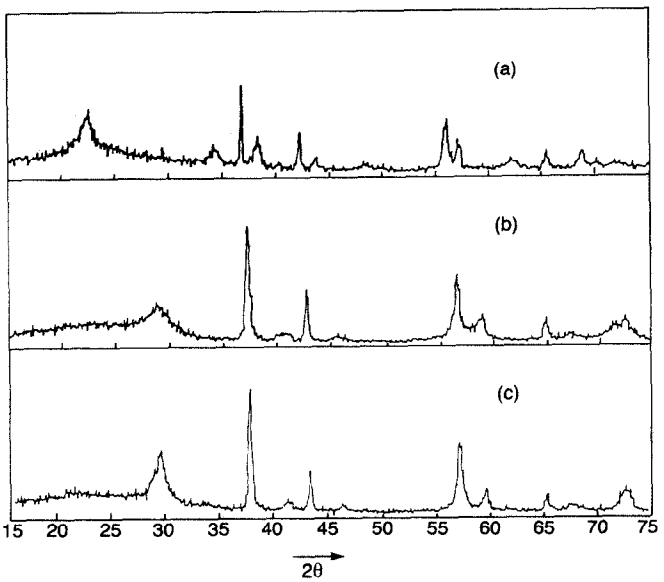

Fig. 2. Powder X-ray diffraction patterns of manganese dioxide samples prepared from $LiMn_2O_4$. (a) γ-MnO_2; (b) β-MnO_2 (after heating (a) to 300 °C); (c) β-MnO_2 (after heating (a) to 350 °C).

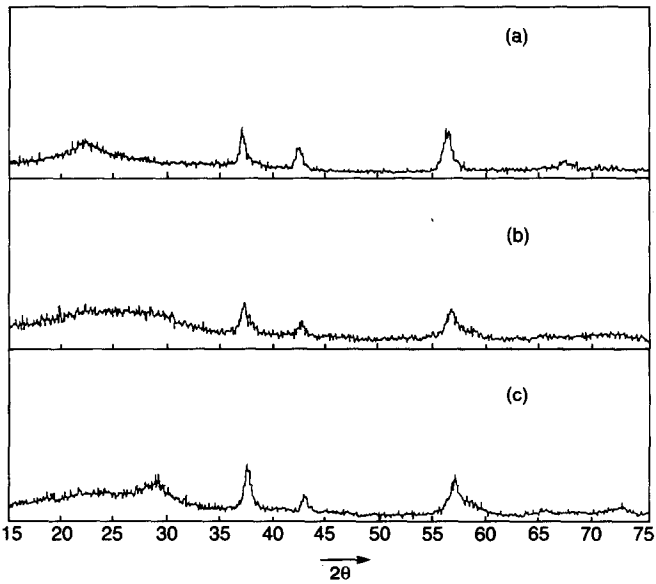

Fig. 3. Powder X-ray diffraction patterns of (a) EMD; (b) "γ/β-MnO_2" (after heating (a) to 350 °C); (c) predominantly β-MnO_2 (after heating (a) to 420 °C).

obtained (Fig. 2(a)). The X-ray pattern in Fig. 2(a) is similar to that reported for other chemically prepared MnO_2 products [16, 17]. This γ-MnO_2 phase is significantly more crystalline than EMD (Fig. 3(a)). The γ-MnO_2 phase, after drying at 75 °C, contains only ~1 wt.% H_2O ($[H^+]$ = 0.13 wt.%). Heat treatment to 300 °C removes the water almost entirely and results in a transformation to β-MnO_2 (Fig. 2(b)). The broad peaks in the pattern are attributed to strain in the individual crystallites. Further heating to 350 °C results in a sharpening of the peaks, indicative of the development of a more crystalline and less strained β-MnO_2 product (Fig. 2(c)). The X-ray pattern of a well-developed β-MnO_2 phase is shown in Fig. 1(c) for comparison.

By contrast, EMD materials contain appreciably more water than the γ-MnO_2 phase described above, as reflected by their $[H^+]$ concentration (0.5 wt.% $[H^+]$). When heated to 350 °C - 420 °C, EMD loses between 80 and 86% of its water. The powder X-ray pattern of EMD heated to 420 °C (Fig. 3(c)) resembles that of the initial EMD phase (Fig. 3(a)), but clearly shows the onset of β-MnO_2 formation, as indicated by the broad peak at 28° 2θ; these results are consistent with published data for EMD [1].

The electrochemical discharge behaviour of lithium cells containing β-MnO_2 cathodes derived from the $LiMn_2O_4$ spinel is compared with the performance of cells containing γ/β-MnO_2 cathodes from heat treated EMD, and with a standard β-MnO_2 product (Fig. 4). Cells with EMD cathodes, whether heated at 350 °C or 420 °C, delivered a capacity equivalent to the uptake of 0.59 Li^+ ions per MnO_2 (182 mA h g^{-1}) when discharged to a cut-off voltage of 2.5 V. A cell containing the standard β-MnO_2 cathode with a

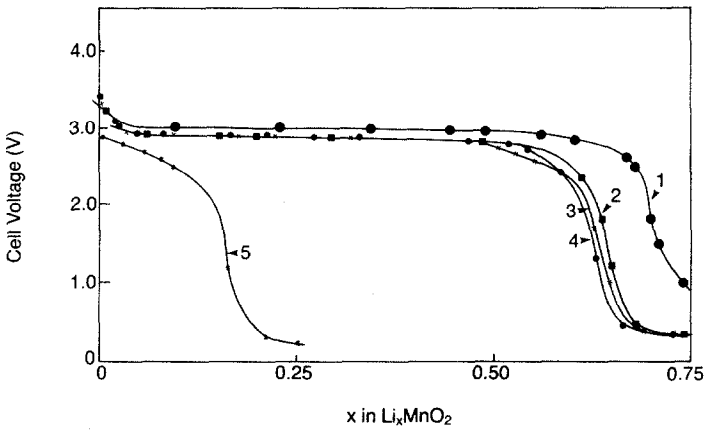

Fig. 4. Discharge characteristics of various Li/MnO_2 cells (30 $\mu A\ cm^{-2}$). 1, Spinel-derived β-MnO_2 heated at 300 °C; 2, spinel-derived β-MnO_2 heated at 420 °C; 3, EMD, heated at 350 °C; 4, EMD, heated at 420 °C; 5, β-MnO_2 from $Mn(NO_3)_2$.

highly developed structure gave a very poor capacity (0.21 Li^+/MnO_2, 65 mA h g^{-1}), which is consistent with earlier reports [10, 11]. However, β-MnO_2 cathodes derived from $LiMn_2O_4$ gave surprisingly high capacities. A cell containing a cathode, heated to 350 °C, discharged at the same voltage as an Li/EMD cell (2.9 V) and delivered a marginally superior capacity (0.61 Li^+/MnO_2, 188 mA h g^{-1}); cathodes heated to 300 °C discharged at a slightly higher voltage (3.0 V), but provided a significantly enhanced capacity (0.68 Li^+/MnO_2, 210 mA h g^{-1}).

Reaction of spinel-derived β-MnO_2 and heat treated EMD samples with an excess of n-butyllithium at room temperature showed that both compounds react readily with one Li^+ ion per MnO_2 unit. With heat treated EMD, one lithium is inserted into the γ/β-MnO_2 structure to yield the lithiated product, $LiMnO_2$. Lithium insertion causes a shift of the peaks in the X-ray pattern of EMD to lower 2θ values, indicative of an expansion of the EMD lattice [2]. However, powder X-ray diffraction patterns of lithiated β-MnO_2 samples showed an amorphous "$LiMnO_2$" product which could not be characterized. It is relevant to mention, however, that the reaction of a highly crystalline β-MnO_2 product with an excess of n-butyllithium at 50 °C yields the lithiated spinel phase $Li_2[Mn_2]O_4$ [18]. A mechanism for the transformation of lithiated β-MnO_2 to spinel has been proposed; it involves a lithium insertion reaction, which is accompanied by a shear of the distorted hexagonal-close-packed oxygen lattice in rutile to the cubic-close-packed lattice in spinel, and a migration of one half of the manganese ions to neighbouring octahedral sites. It is conceivable that this process also occurs when the spinel derived β-MnO_2 product is lithiated. The high reactivity of this β-MnO_2 phase (both chemical and electrochemical) compared with a highly crystalline β-MnO_2 phase can be largely attributed to its small average particle size (7.5 μm) and to the strain in the particles. The

TABLE 2

Particle-size distribution in $LiMn_2O_4$, γ-MnO_2, and EMD (Delta) samples

$LiMn_2O_4$		γ-MnO_2		EMD	
Size band (μm)	%	Size band (μm)	%	Size band (μm)	%
118.4 - 54.9	0.0	118.4 - 54.9	0.0	564.0 - 261.7	0.2
54.9 - 33.7	2.5	54.9 - 33.7	0.0	261.7 - 160.4	2.9
33.7 - 23.7	28.7	33.7 - 23.7	0.0	160.4 - 112.8	7.0
23.7 - 17.7	32.7	23.7 - 17.7	0.0	112.8 - 84.3	9.6
17.7 - 13.6	19.0	17.7 - 13.6	0.4	84.3 - 64.6	10.8
13.6 - 10.5	9.3	13.6 - 10.5	9.8	64.6 - 50.2	11.0
10.5 - 8.2	4.3	10.5 - 8.2	28.5	50.2 - 39.0	10.7
8.2 - 6.4	2.0	8.2 - 6.4	28.5	39.0 - 30.3	9.6
6.4 - 5.0	0.9	6.4 - 5.0	17.4	30.3 - 23.7	8.3
5.0 - 3.9	0.4	5.0 - 3.9	8.6	23.7 - 18.5	6.9
3.9 - 3.0	0.2	3.9 - 3.0	3.8	18.5 - 14.5	5.5
3.0 - 2.4	0.1	3.0 - 2.4	1.7	14.5 - 11.4	4.3
2.4 - 1.9	0.0	2.4 - 1.9	0.7	11.4 - 9.0	3.3
1.9 - 1.5	0.0	1.9 - 1.5	0.3	9.0 - 7.2	2.5
1.5 - 1.2	0.0	1.5 - 1.2	0.1	7.2 - 5.8	1.9
Mean particle size = 20.4 μm		Mean particle size = 7.5 μm		Mean particle size = 41.1 μm	

amorphous nature of the lithiated product is attributed to an extremely small particle size, which results from the break up of the strained β-MnO_2 particles during lithiation.

Particle-size distributions of typical EMD, $LiMn_2O_4$ and γ-MnO_2 (ex $LiMn_2O_4$) samples used in this investigation are compared in Table 2. It is noteworthy that the mean particle size of γ-MnO_2 (7.5 μm) is significantly smaller than that of EMD (41.1 μm). Note also that the mean particle size of γ-MnO_2 is appreciably smaller than that of the $LiMn_2O_4$ parent material (20.4 μm); the reduction in particle size is a result of the dissolution of Mn^{2+} ions during the formation of the λ-MnO_2 precursor according to the reaction [3]:

$$2LiMn_2O_4 \longrightarrow Li_2O + 3MnO_2 + MnO$$

The cycling behaviour of spinel-derived β-MnO_2 and heat treated (360 °C) EMD I.C.1 cathodes, containing TAB, in cells operated at 1 mA cm^{-2} (charge and discharge) is compared in Fig. 5. These cathodes yielded an initial discharge capacity of 206 mA h g^{-1} MnO_2 (0.67 Li^+/MnO_2) and 208 mA h g^{-1} (0.68 Li^+/MnO_2), respectively. The cells lost capacity rapidly on cycling, as expected.

Li^+-ion diffusion rates ($\tilde{D}$) in heat treated, spinel-derived γ-MnO_2 and β-MnO_2 phases were determined to be significantly higher than in corresponding heat treated, standard EMD and β-MnO_2 phases. For example, for a

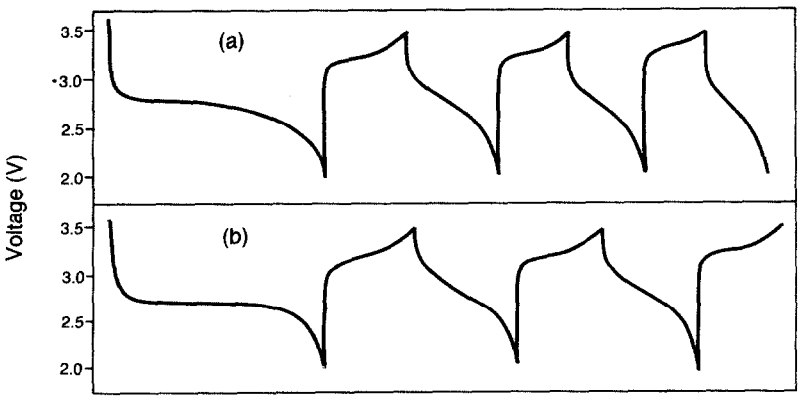

Fig. 5. Cycling behaviour of Li/MnO_2 cells (1 mA cm^{-2} discharge and charge). (a) Spinel-derived β-MnO_2, heated at 300 °C; (b) EMD (I.C.1, heated at 360 °C).

spinel-derived γ-MnO_2 phase that had been heated to 200 °C ($[H^+]$ = 0.09 wt.%), $\tilde{D} = 1 \times 10^{-9}$ cm^2 s^{-1} in contrast to $\tilde{D} = 9 \times 10^{-11}$ cm^2 s^{-1} for a heat treated EMD sample ($[H^+]$ = 0.10 wt.%). $\tilde{D}$ values for the anhydrous β-MnO_2 phases derived from $LiMn_2O_4$ and $Mn(NO_3)_2$ were 2×10^{-10} cm^2 s^{-1} and 6×10^{-11} cm^2 s^{-1}, respectively. The value of $\tilde{D}$ obtained in this work for the standard samples of EMD and β-MnO_2 compare well with data reported elsewhere, *viz.*, 3×10^{-10} cm^2 s^{-1} [19] and 3×10^{-11} cm^2 s^{-1} [20], respectively.

Acknowledgement

Mr Steve Swart of Delta (EMD) (Pty) Ltd, is thanked for undertaking the particle-size analyses. Mr H. Lachmann of the National Chemical Research Laboratory, CSIR, is thanked for the hydrogen-ion analyses.

References

1 H. Ikeda, *U.S. Pat. 4,133,856.*
2 H. Ikeda and S. Narukawa, *J. Power Sources, 9* (1983) 329.
3 J. C. Hunter, *J. Solid State Chem., 39* (1981) 142.
4 M. M. Thackeray, W. I. F. David, P. G. Bruce and J. B. Goodenough, *Mater. Res. Bull., 18* (1983) 461.
5 A. Mosbah, A. Verbaere and M. Tournoux, *Mater. Res. Bull., 18* (1983) 1375.
6 W. I. F. David, M. M. Thackeray, L. A. de Picciotto and J. B. Goodenough, *J. Solid State Chem., 67* (1987) 316.
7 J. C. Hunter and F. B. Tudron, *Proc. Electrochem. Soc., 85*(4) (1985) 441.
8 M. M. Thackeray, P. J. Johnson, L. A. de Picciotto, P. G. Bruce and P. G. Goodenough, *Mater. Res. Bull., 19* (1984) 179.
9 M. M. Thackeray and A. de Kock, *J. Solid State Chem., 74* (1988) 414.

10 G. Pistoia, *J. Power Sources, 9* (1983) 307.
11 D. W. Murphy, F. J. Di Salvo, J. N. Carides and J. V. Waszczak, *Mater. Res. Bull., 13* (1978) 1395.
12 S. Basu and W. L. Worrell, in P. Vashishta, J. N. Mundy and G. K. Shenoy (eds.), *Fast Ion Transport in Solids*, North-Holland, Amsterdam, 1979, p. 149.
13 M. M. Thackeray, W. I. F. David and J. B. Goodenough, *Mater. Res. Bull., 17* (1982) 785.
14 G. Pistoia, M. Pasquali, M. Tocci, V. Manev and R. V. Moshtev, *J. Power Sources, 15* (1985) 13.
15 T. Hirai and I. Tari, *Prog. Batteries Solar Cells, 3* (1980) 157.
16 W. K. Zwicker, W. O. J. Groeneveld Meijer and H. W. Jaffe, *Am. Mineral., 47* (1962) 246.
17 *JCPDS Powder X-ray diffraction file: 14-644.*
18 W. I. F. David, M. M. Thackeray, P. G. Bruce and J. B. Goodenough, *Mater. Res. Bull., 19* (1984) 99.
19 J. Vondrák, I. Jakubec and J. Bludska, *J. Power Sources, 14* (1985) 141.
20 A. Zamouche and F. Dalard, *Ext. Abstr., 6th Int. Conf. Solid State Ionics, Garmisch Partenkirchen, F.R.G., Sept. 6 - 11, 1987*, p. 627.